Investigation of Energy Deposited by Femtosecond Electron Transfer in Collisions Using Hydrated Ion Nanocalorimetry

Anne I. S. Holm,[†] William A. Donald,[‡] Preben Hvelplund,*[,†] Mikkel K. Larsen,[†] Steen Brøndsted Nielsen,*[,†] and Evan R. Williams*[,‡]

Department of Physics and Astronomy, University of Aarhus, Denmark, and Department of Chemistry, University of California, Berkeley, California 94720-1460

Received: March 5, 2008; Revised Manuscript Received: August 11, 2008

Ion nanocalorimetry is used to investigate the internal energy deposited into $M^{2+}(H_2O)_n$, M = Mg (n = 3−11) and Ca (n = 3−33), upon 100 keV collisions with a Cs or Ne atom target gas. Dissociation occurs by loss of water molecules from the precursor (charge retention) or by capture of an electron to form a reduced precursor (charge reduction) that can dissociate either by loss of a H atom accompanied by water molecule loss or by exclusively loss of water molecules. Formation of bare $CaOH^+$ and Ca^+ by these two respective dissociation pathways occurs for clusters with n up to 33 and 17, respectively. From the threshold dissociation energies for the loss of water molecules from the reduced clusters, obtained from binding energies calculated using a discrete implementation of the Thomson liquid drop model and from quantum chemistry, estimates of the internal energy deposition can be obtained. These values can be used to establish a lower limit to the maximum and average energy deposition. Not taking into account effects of a kinetic shift, over 16 eV can be deposited into $Ca^{2+}(H_2O)_{33}$, the minimum energy necessary to form bare $CaOH^+$ from the reduced precursor. The electron capture efficiency is at least a factor of 40 greater for collisions of $Ca^{2+}(H_2O)_9$ with Cs than with Ne, reflecting the lower ionization energy of Cs (3.9 eV) compared to Ne (21.6 eV). The branching ratio of the two electron capture dissociation pathways differs significantly for these two target gases, but the distributions of water molecules lost from the reduced precursors are similar. These results suggest that the ionization energy of the target gas has a large effect on the electron capture efficiency, but relatively little effect on the internal energy deposited into the ion. However, the different branching ratios suggest that different electronic excited states may be accessed in the reduced precursor upon collisions with these two different target gases.

Introduction

Fast (multi-kiloelectronvolt) ion−atom collisions are used in tandem mass spectrometry for characterizing ionic structures,[1,2] studying the structures and stabilities of unusual neutral species,[1−14] and, more recently, investigating structures of multiply charged peptides and proteins.[15−18] Collisions between ions and atoms can result in ion activation and also electron transfer. The latter process has been extensively used in neutralization reionization mass spectrometry experiments to prepare unusual neutral species from corresponding ions, with subsequent ionization of the neutral species accomplished by a second collision.[2−8] The second collision can produce either positive or negative ions, making it possible to perform charge reversal experiments.[9,10,19] The latter experiments have been recently used to investigate the stabilities of neutral radicals formed by collisional electron capture of singly charged peptide ions with Cs.[19] In these experiments, anions formed from neutral z fragments were observed, whereas the c anions were not formed. This result was attributed to a carbanion formation of a stable z anion vs a reactive radical for the c ion that has a lifetime of less than a few microseconds.

An advantage of electron capture induced dissociation (ECID) from an atomic or molecular target for ions with two or more charges is that the product ions formed by capture of a single electron can be detected directly.[15−18,20] ECID experiments have been used to investigate the structures of peptides and proteins,[15−18] and fragmentation similar to electron capture dissociation (ECD) experiments,[21−29] in which multiply charged ions capture a free electron, is observed. The ECID experiments have the advantage that reactions that occur on a short time scale (a few microseconds) can be investigated. This method was used to study the H atom loss from multiply charged peptide ions and the role of hydrogen bonding and microsolvation on the reduced precursor stability and fragmentation pathways.[18] For example, the ratio of $(M + H)^+$ to $(M + 2H)^{\bullet+}$ was found to decrease when doubly protonated di- and tripeptides were solvated with one or more methanol molecules upon electron transfer from Na.[18] The increased abundance of the latter ion was attributed to a solvent "caging" effect. Recent experiments with ^{15}N-labeled peptides demonstrate that ammonia loss occurs from the N-terminus,[15] consistent with predictions from theory.[30]

Experimental results from high-energy (10 keV) collisions between $Cu^{2+}(H_2O)_n$ and Xe gas were recently reported by Stace and co-workers.[31] The major fragmentation pathway is loss of water molecules from the mass-selected precursor, but fragment ions formed by ECID were also observed. In this latter process, two fragmentation processes occur in which the reduced precursor either lost exclusively water molecules or lost a H

* To whom correspondence should be addressed. E-mail: Hvelplun@phys.au.dk (P.H.); sbn@phys.au.dk (S.B.N.); Williams@cchem.berkeley.edu (E.R.W.).
[†] University of Aarhus.
[‡] University of California.

10.1021/jp8019655 CCC: $40.75
Published on Web 10/04/2008

atom and water molecules. Similar dissociation pathways have been reported in ECD spectra of $M^{2+}(H_2O)_n$, M = Mg and Ca.[32]

An important parameter for characterizing any fragmentation method is the internal energy that is deposited into an ion upon activation. In ECID experiments, electron transfer from the target gas to the ion can be endothermic or exothermic depending on the relative ionization energies of the reduced ion and target gas. In addition, a significant amount of energy can be transferred in the collision process itself. For example, the center-of-mass collision energy between a doubly charged cation of mass 200 Da with 100 keV of kinetic energy and a Cs atom is 39.9 keV. A measure of the internal energy deposition into an ion can be obtained using "chemical thermometers", which are ions that have known dissociation energies and entropies.[33−43] Metal carbonyl complexes that have known fragment appearance energies have been used to investigate the internal energy deposition from a variety of activation methods.[33−36] For example, Cooks and co-workers first characterized the energy deposited into $W(CO)_6^{2+}$ upon charge exchange with a series of atomic and molecular targets (from toluene, IE = 8.8 eV, to He, IE = 24.6 eV) at both high (15.6 keV[33] and 7 keV[34]) and low (0−50 eV[35]) collision energies. Charge exchange at high collision energies resulted in broad energy distributions, the average of which were weakly correlated with the ionization energy of the target. W^{2+} was observed, indicating that up to 15 eV was deposited. These observations support a close approach mechanism for high-energy charge exchange in which significant collisional energy is deposited into the ion. A measure of the energy deposited into $W(CO)_6^{2+}$ upon electron transfer in 10 keV collisions with Ar, K, and Cs has been recently reported.[37,38]

An alternative approach to measure internal energy deposited by electron capture, or any other activation method, uses solvated ions as nanocalorimeters.[32,44−48] This method has been demonstrated with hydrated di- and trivalent ions and has been used to measure the internal energy deposition in ECD experiments as a function of the cluster size and metal ion identity. In brief, activation of a hydrated ion results in evaporation of water molecules from the cluster. The extent of activation can be estimated from the sum of the threshold dissociation energies for the maximum number of water molecules lost. This method has the advantages that the binding energies of water molecules to a highly hydrated ion are significantly less than the binding energies of CO molecules to metal ions, and potentially many water molecules can be lost from large clusters. Thus, hydrated metal ions can provide significantly improved resolution, accuracy, and range in determining the internal energy distributions. Threshold dissociation energies for the loss of water molecules from large clusters can be obtained from calculations of binding energies derived from the Thomson liquid drop model (TLDM).[49,50] For smaller clusters, dissociation energies from experimental measurements or quantum chemical calculations can be used.[32] A more accurate method to obtain information about energy deposition in nanocalorimetry can be obtained from the average number of water molecules lost and estimates of energy lost to the products in the form of translational, vibrational, and rotational energy.[44] This method has been used to accurately measure recombination energies upon electron capture by hydrated ions.[44] Recombination energies of large clusters can be related to relative reduction enthalpies measured in aqueous solution.[44,46] Measurements of a variety of redox-active species in nanodrops have recently been used to obtain a measure of the absolute potential of the standard hydrogen electrode.[44]

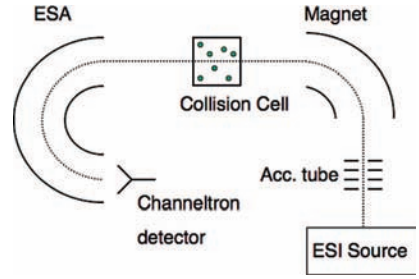

Figure 1. Sector mass spectrometer at Aarhus used for electron capture induced dissociation experiments. See the text for details.

Here, data from ECID experiments done with 100 keV collisions between $M^{2+}(H_2O)_n$, M = Mg (for n = 3−11) and Ca (for n between 3 and 33), and Cs are used to obtain a measure of the internal energy deposited upon collisional energy transfer. The effects of ion size on energy deposition over a range of masses relevant to previously investigated peptides are investigated. The results presented here demonstrate that the energy deposition in ECID can be significantly broader and much higher than that obtained by ECD, indicating that both the collision process and the different time frames of these two experiments result in significant differences in the observed fragmentation.

Experimental Section

The experimental apparatus at Aarhus is described in detail elsewhere.[51,52] Hydrated divalent metal ions were generated by electrospray from aqueous solutions containing dissolved MCl_2, where M corresponds to Mg or Ca, using a syringe-pump system to regulate solution flow to a rate of 1−2 μL/min. The resulting ions are introduced into a sector mass spectrometer through an electrospray interface, accelerated by a 50 kV potential (corresponding to 100 keV ion kinetic energies), m/z selected by a magnet (∼1000 resolution), and passed through a heated cesium vapor cell (Figure 1). The interaction between a reacting cluster and the cesium or neon atoms occurs within a few femtoseconds, during which time an electron from the 6s orbital of a cesium atom can be transferred to the doubly charged cluster ion. Because of the short interaction time, the transition should be a vertical or nearly vertical process, but energy redistribution and fragmentation can occur during the flight time prior to mass analysis. Positive fragment ions resulting from these collisions are analyzed using a hemispherical electrostatic analyzer (ESA). The dissociation time scale corresponds to the ion flight time from the collision cell to the ESA, which for clusters ranging from 3 to 33 water molecules, is in the range of 3−6 μs. A two-point linear calibration between analyzer voltage and ion mass was performed by setting zero voltage to zero m/z and setting the voltage difference between the two analyzer plates (2 × 5.17 kV) to the m/z of the precursor ion. Peak areas were divided by ion masses to correct for the spectrometer efficiency.[53] Corrections for a mass-dependent detector efficiency were not done, but they are believed to be small.

The uncertainty in the average number of water molecules lost and the branching ratio is ∼1% for the smaller clusters (n ≤ 15) and ∼5% for the larger ones. The criteria for establishing a detection limit were that there must be a signal in at least two adjacent detection channels and the maximum signal must be 2 times greater than the average noise level determined over a neighboring 10 Da range. The detection channel widths are 1024/(2 × precursor m/z), 2048/(2 × precursor m/z), and 4096/(2 × precursor m/z) for n = 3−13, n = 15−19, and n = 21−33, respectively. Efficiencies for various dissociation processes were

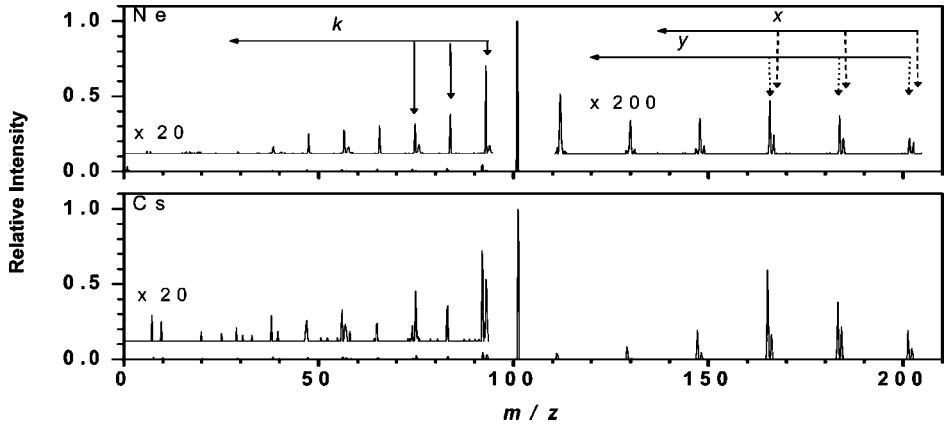

Figure 2. Mass spectra obtained upon collision between $Ca^{2+}(H_2O)_9$ and Ne (top) or Cs (bottom), where *k*, *x*, and *y* correspond to the number of water molecules lost by charge retention and charge reduction via pathways I and II, respectively.

calculated from the sum of ion intensities for that process divided by the overall ion signal.

Results and Discussion

Fragmentation Pathways. Collisions (100 keV) of $Ca^{2+}(H_2O)_n$ with either Ne or Cs as a target gas result in dissociation by three different pathways:

charge retention

$$Ca^{2+}(H_2O)_n + Cs \rightarrow Ca^{2+}(H_2O)_{n-k} + kH_2O + Cs$$

charge reduction

$$Ca^{2+}(H_2O)_n + Cs \rightarrow Ca^{+}(H_2O)_{n-x} + xH_2O + Cs^{+} \quad \text{(pathway I)}$$

$$Ca^{2+}(H_2O)_n + Cs \rightarrow CaOH^{+}(H_2O)_{n-y-1} + yH_2O + H + Cs^{+} \quad \text{(pathway II)}$$

The precursor can be activated by the collision, resulting in the loss of one or more water molecules and remain doubly charged (charge retention), or the precursor can be reduced by transfer of an electron from the target gas. The latter ECID process can result in either loss of water molecules exclusively (pathway I) or ejection of a H atom and loss of water molecules, resulting in formation of a hydrated metal hydroxide (pathway II). These ECID pathways are the same as those previously observed in ECID of $Cu^{2+}(H_2O)_n$, $n = 4-16$,[31] and those observed by ECD of $Ca^{2+}(H_2O)_n$, $n = 4-47$.[32] Neither protonated water nor protonated water clusters are observed. Thus, the charge separation reaction, $Ca^{2+}(H_2O)_n \rightarrow CaOH^{+}(H_2O)_{n-j-1} + H^{+}(H_2O)_j$, that is observed for some hydrated divalent metal ions upon activation does not occur under these conditions.[54,55] This is consistent with the loss of neutral water molecules being entropically favored over the charge separation reaction as is the case for $SO_4^{2-}(H_2O)_n$.[56]

Product ions formed by the three possible dissociation pathways are shown in the ECID spectra of $Ca^{2+}(H_2O)_9$ with either Ne or Cs in Figure 2 (top and bottom, respectively). Fragment ions originating from charge retention and charge reduction via pathways I and II are denoted by *k*, *x*, and *y*, respectively. For the charge retention pathway, the distribution and intensities of the fragment ions for both target gases are very similar. However, the charge reduction channel is 40 times greater for Cs than for Ne, reflecting the lower ionization energy of Cs (3.9 eV) vs Ne (21.6 eV). Collision with residual O_2 gas ($IE_{O_2} = 13.6$ eV) in the beam path can also result in electron transfer, so the 40-fold greater electron transfer with Cs compared to Ne is a lower limit. The distributions of product ions formed upon collision with both target gases are similar with respect to water loss, but differ significantly in the branching ratio of the two charge reduction pathways. The ratio of pathway I to pathway II is 1:9 with neon, whereas this ratio for Cs is 1:3. The different branching ratios for pathways I and II could be due to a different population of electronic excited states that are accessed for each of the two target gases. These results indicate that the ionization energy of the target gas plays a major role in the electron capture dissociation efficiency, but a relatively minor role in the average distribution of internal energy deposition. Additional nanocalorimetry experiments with different target gases should provide useful information about the role of excited-state chemistry on these and other ECID pathways.

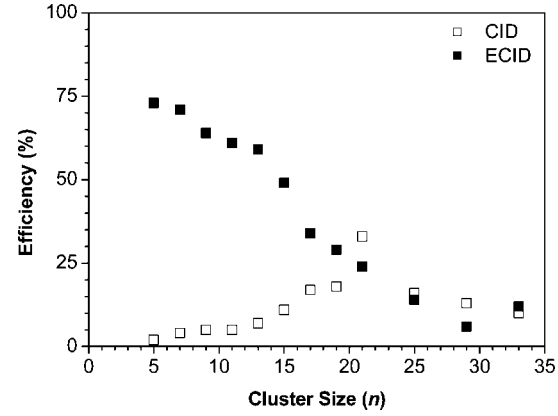

Figure 3. Charge retention (open squares) and charge reduction (solid squares) efficiencies upon collision between $Ca^{2+}(H_2O)_n$ and Cs.

Fragmentation Efficiency. The extent of fragmentation resulting from these 100 keV collisions depends on a number of experimental parameters, including the target gas identity and pressure, ion kinetic energy, and cluster size. To investigate the effects of the cluster size on the fragmentation efficiency, experiments in which all other parameters remain constant were performed. For the combined ECID pathways, the efficiency of fragmentation is highest for the smaller clusters (>70%) and decreases significantly with increasing cluster size to a value of ~13% for $Ca^{2+}(H_2O)_{33}$ (Figure 3, solid squares). In contrast, the efficiency for producing fragment ions by the charge retention pathway is ~4% at the smallest cluster size, increases to ~35% at $n = 21$, and decreases with increasing cluster size (Figure 3, open squares).

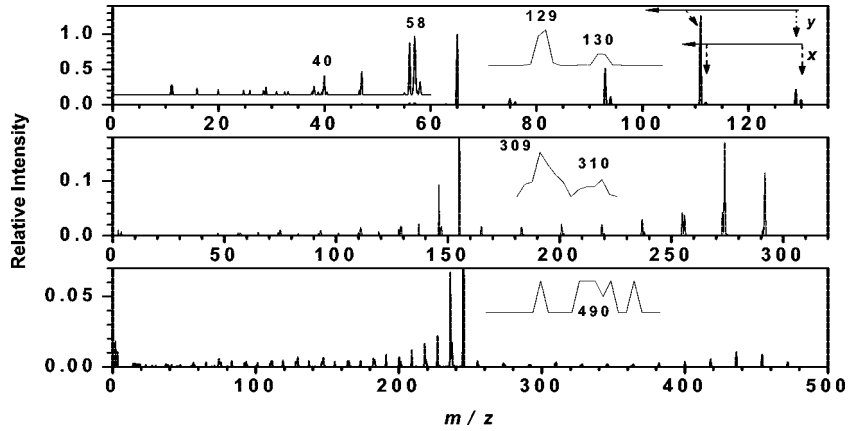

Figure 4. Mass spectra obtained upon collision between $Ca^{2+}(H_2O)_n$, $n = 5$ (top), $n = 15$ (middle), or $n = 25$ (bottom), and Cs. The charge-reduced ions $Ca^{+}(H_2O)_5$ (*m/z* 130) and $Ca^{+}(H_2O)_{15}$ (*m/z* 310) as well as those that have lost a H atom (*m/z* 129 and 309) are clearly detected (cf. the insets), whereas $Ca^{+}(H_2O)_{25}$ (*m/z* 490) and the corresponding H-loss ion (*m/z* 489) are at the limit of detection. A 30-fold expansion of the lower mass region of the top spectrum shows that Ca^{+} (*m/z* 40) and $Ca^{+}(OH)$ (*m/z* 58) are formed.

The increasing charge retention efficiency with increasing cluster size for $n \leq 21$ is indicative of an increasing geometrical cross section (the larger the cluster, the bigger the impact parameter). However, the number of degrees of freedom (DOF) increases with increasing cluster size as well. For a given internal energy deposition, the observed fragmentation will decrease with increasing cluster size because this energy is distributed over more internal modes so that less fragmentation will occur in the limited time frame of these experiments.[57] This DOF effect is dominant for the larger clusters. For ECID, the monotonic decrease in efficiency with increasing cluster size likely reflects increased shielding or delocalization of the charge by the additional water molecules. Increased shielding or delocalization should decrease the Coulomb attraction with increasing cluster size. The propensity for electron transfer to larger hydrated anionic nucleotide clusters increases with increasing size (up to $n = 16$), and this phenomenon is likely due to charge shielding and delocalization as well.[58] In this case, the Coulomb repulsion should decrease with size.

Reactivity as a Function of the Cluster Size. In addition to the strong dependence of the ECID efficiency on cluster size, there is also a strong dependence of the branching ratio for pathways I and II on the cluster size. This effect is illustrated in Figure 4, which shows the ECID spectra for $Ca^{2+}(H_2O)_n$, $n = 5$, 15, and 25, with the product ions formed by pathways I and II indicated by *x* and *y*, respectively, in these spectra. The distributions of product ions formed by both pathways are very broad and result in cluster ions that range from the charge-reduced precursor all the way down to bare $CaOH^+$ and, for $n \leq 17$, the completely desolvated Ca^+. The breadth of the distribution reflects the broad range of internal energies that can be deposited in the collision process, and the formation of bare Ca^+ and $CaOH^+$ indicates that the maximum energy deposition is quite high.

The formation of Ca^+ from the larger reduced clusters is surprising because of the large internal energy deposition necessary to evaporate all the water molecules from the cluster and because the competitive formation of $CaOH^+$ is energetically favored at small cluster sizes.[32] The appearance of Ca^+ in these experiments indicates that loss of water molecules is kinetically favored over loss of a H atom at the smaller cluster sizes.

A rough estimate of the minimum energy necessary to form the bare ions from the reduced precursor can be obtained from the sum of threshold dissociation energies for all the water molecules that evaporate from the reduced cluster. Because threshold dissociation energies have not been measured for the larger clusters investigated in this study, binding energies calculated using a discrete TLDM were used.[49] It has recently been demonstrated that a discrete implementation of this model can accurately reproduce both experimental and quantum chemical values for smaller mono- and divalent hydrated ions.[49] Values obtained from quantum chemical calculations were used for the smaller clusters ($n \leq 6$).[32]

Formation of the bare calcium ion via pathway I is observed from reduced precursors with up to 17 water molecules. The sum of the threshold dissociation energies for loss of 17 water molecules from $Ca(H_2O)_{17}^+$ is ~9.6 eV (221 kcal/mol). Formation of $CaOH^+$ from pathway II is observed for clusters with up to 33 water molecules. Evaporation of water from $Ca(H_2O)_{33}^+$ requires a minimum of 15.6 eV (360 kcal/mol), not including any energy required to eject a H atom from the reduced cluster. These internal energy deposition values are the minimum necessary to form the smallest ions via these two pathways. These values do not include effects of a kinetic shift in which much more internal energy must be deposited to produce this extent of fragmentation over the limited time scale ($3 - 6$ μs) available for dissociation prior to fragment mass analysis by the ESA.

For ECID of $Cu^{2+}(H_2O)_n$, $n = 4-16$, the distribution of product ions is narrower with only four to five fragment ions formed from the reduced precursor.[31] In addition, the intact charge-reduced precursor is rarely observed, and there is no evidence of bare Cu^+.[31] The broader distribution observed here may be due to the higher signal-to-noise ratio in our experiments, which enables detection of much lower abundance ions and also the higher collision energy (100 keV vs 10 keV), although different target gases may also play a role.

The ECID results are in sharp contrast to those obtained by ECD of $Ca^{2+}(H_2O)_n$, where only a few product ions formed by each dissociation pathway are observed, indicating that a very narrow range of internal energy is deposited into the precursor upon capture of a free electron.[32,45] For example, capture of a free electron by $Ca^{2+}(H_2O)_{24}$ results in just one fragment ion by pathway I ($Ca^{+}(H_2O)_{14}$) and three product ions by pathway II ($CaOH^{+}(H_2O)_n$, $n = 12-14$), although the lower signal-to-noise ratio in the ECD experiments has a minor effect on this comparison.[32] In ECD, the time scale for dissociation is tens to hundreds of milliseconds and can be readily extended to several

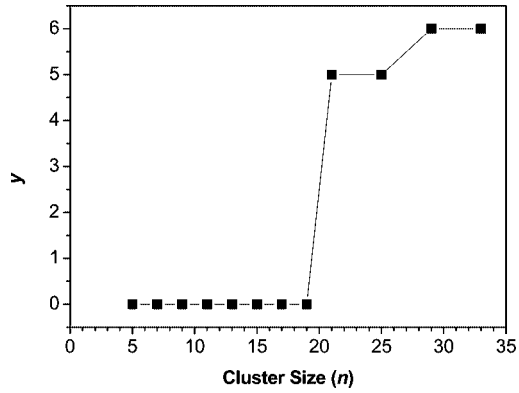

Figure 5. Minimum number of water molecules lost from pathway II, y, upon ECID of $Ca^{2+}(H_2O)_n$ with a Cs target as a function of the cluster size.

seconds so that kinetic shift effects are negligible. In addition, capture of an electron is most efficient when the relative energy between the ion and electron approaches zero so that the internal energy deposition depends only on the recombination energy (or adiabatic ionization energy of the reduced precursor) and not on the electron kinetic energy under typical experimental conditions where low-energy electrons are used.[48]

In ECID, transfer of the electron from the target requires an energy corresponding to the ionization energy of the target gas ($IE_{Cs} = 3.9$ eV, $IE_{Xe} = 12.0$ eV, $IE_{Ne} = 21.6$ eV), making the process less exothermic than capture of a free electron by this corresponding value. However, energy from the collision itself can be transferred into the ion. The comparison of results from ECID and ECD for $Ca^{2+}(H_2O)_n$ indicates that this collisional energy transfer is substantial and accounts for the much broader distribution of product ions observed using ECID.

For clusters with up to 19 water molecules, all possible fragments originating from pathway II are observed ($y = 0$ to $n - 1$). Surprisingly, the larger fragment ions corresponding to loss of zero to five or six water molecules ($y = 0$ to 4 or 5) formed by pathway II are missing for clusters with 20 or more water molecules. Data for the *minimum* number of water molecules lost by pathway II are summarized as a function of the cluster size in Figure 5. The absence of the largest of the possible fragment ions for the larger clusters cannot be attributed to fragment ion stability because these same ions are observed for $n \leq 19$! The origin of this phenomenon is unclear, but it may be due to effects of forming a third solvation shell. Transition from pathway II to pathway I in the ECD data starts at clusters with 21 water molecules, suggesting that both effects may be related to the structure of the hydrated cluster.[32]

Interestingly, results for reduced $Cu^{2+}(H_2O)_n$ by Stace and co-workers[31] show an even progression in the minimum number of water molecules lost by pathway II with increasing cluster size, although this comparison is obfuscated by the difficulty in clearly distinguishing these two pathways due to limited product ion resolution. In contrast, fragment ions formed by these two pathways are nearly baseline resolved, even for low-abundance ions in our experiments (Figures 2 and 4).

The ratio between fragmentation by pathway I and that by pathway II obtained from the sum of ion intensities for the product ions formed by these two respective pathways is shown in Figure 6 (solid triangles, pathway I; open triangles, pathway II). Both pathways are observed for all cluster sizes, but pathway II is dominant for smaller clusters ($n < 15$) where ~90% of the ECID fragments are from pathway II for reduced $Ca^{2+}(H_2O)_5$. For larger clusters ($n \geq 15$), the extents of dissociation by the two pathways are comparable.

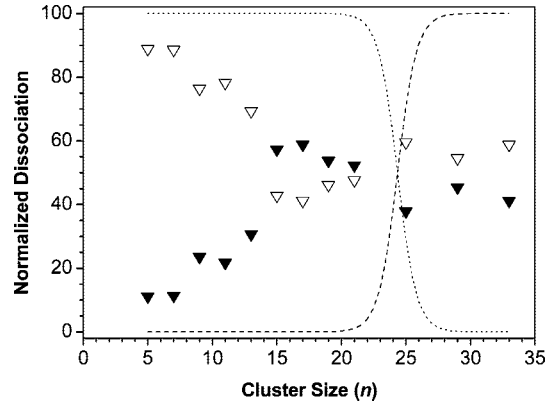

Figure 6. Normalized product ion intensities for dissociation by pathways I (solid triangles) and II (open triangles) resulting from ECID with a Cs target and pathways I (---) and II (•••) resulting from ECD by $Ca^{2+}(H_2O)_n$, $n = 5-33$,[32] as a function of the precursor cluster size.

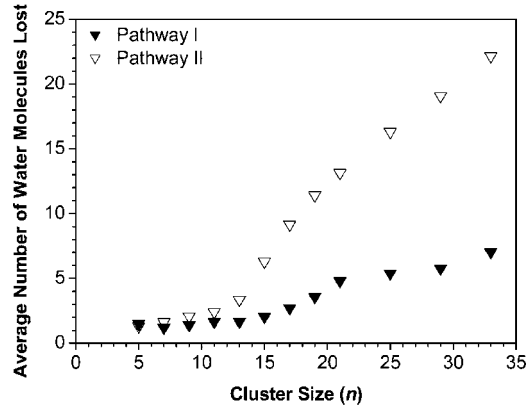

Figure 7. Average number of lost water molecules upon ECID of $Ca^{2+}(H_2O)_n$ by pathways I (solid triangles) and II (open triangles) with a Cs target as a function of the cluster size.

ECID data obtained for $Cu^{2+}(H_2O)_n$ show that both pathways occur for $n < 13$ whereas only fragments formed by pathway II are observed for n up to 16.[31] This difference in reactivity could be due to the different properties of the metal ions or differences in the structures of the clusters. It may also be a consequence of solvent-separated ion−electron pair formation in large reduced clusters of $Ca^{2+}(H_2O)_n$[32] vs direct metal ion reduction in large clusters of $Cu^{2+}(H_2O)_n$.[44,47]

In contrast, the ECD results show that pathway II occurs exclusively for $n \leq 22$ and pathway I occurs exclusively for $n \geq 30$. For $22 < n < 30$, a sharp transition between these two pathways occurs (Figure 6). Although the general trends in ECID and ECD are similar, the much sharper transition between the two reaction pathways observed for ECD can likely be attributed to the much narrower internal energy deposited upon capture of a free electron.

Average Number of Water Molecules Lost. One way to characterize the extent of dissociation as a function of the cluster size is by calculating the average number of water molecules lost via both pathways for each cluster; these data are summarized in Figure 7. The average number of water molecules lost by both pathways is nearly constant for $n \leq 9$ but smoothly increases with larger cluster sizes. By comparison, ECD data show a nearly linear increase in the average number of water molecules lost with increasing cluster size up to $n \approx 25$, after which these data plateau and subsequently decrease for even larger cluster sizes.[32] At small sizes, the binding energy of water

increases with decreasing cluster size so that, for a given internal energy deposition, fewer water molecules are lost. This effect dominates over any increase in RE expected for smaller clusters. The plateau in the ECD data and subsequent decrease in the average number of water molecules lost with increasing cluster size can be explained predominantly by increased ion solvation resulting in a lower recombination energy, although other effects may play a role as well.[32]

The trend in the beginning of the ECID data (Figure 7) can be explained by the large amount of energy that is deposited into these small clusters. Fragments corresponding to evaporation of all water molecules (forming Ca^+ and $CaOH^+$ by pathways I and II, respectively) are observed for these smaller clusters. Energy in excess of that required to form the bare ions can appear as translational, rotational, and vibrational excitation of the products; e.g., $CaOH^+$ can be highly excited.

The absence of a maximum in the ECID data over this range in cluster size is interesting given that there is a plateau in the ECD data for $n = 25-32$ and a decrease for even larger clusters.[32] This phenomenon cannot be ascribed to a DOF effect because longer dissociation time scales would result in an even higher average water molecule loss. Both the center-of-mass collision energy and the velocity of the ions decreases with increasing cluster ion size, and both may have an effect on the internal energy deposited by electron transfer. However, the effect of the water binding energy as a function of the cluster size has a greater effect on the ECID data because of the very broad distribution of product ions formed.

Average Internal Energy Deposition. From the average number of water molecules lost from the reduced precursor ions, it is possible to obtain a rough estimate of how the average internal energy deposition changes as a function of the cluster size. The average number of water molecules lost is only a rough measure of energy deposition due to the broad distribution of product ions observed. Moreover, the appearance of product ions depends both on the threshold energy necessary for ion formation and on the excess energy above this value necessary to observe dissociation on the time scale of these experiments. This latter effect, i.e., a kinetic shift, becomes increasingly important with increasing cluster size because of the DOF effect.

Using the sequential water binding energies for $Ca^+(H_2O)_n$ calculated using a discrete implementation of the TLDM[49] and quantum chemical values for the smaller clusters ($n \leq 6$),[32] and a weighted average number of water molecules lost by combined pathways I and II, information about the average energy deposition as a function of the cluster size can be obtained. This analysis does not include the effects of a kinetic shift, it does not account for any endothermicity associated with formation of a hydrogen atom by pathway II, and it does not include the effects of the distribution width. A comparison of results from these ECID experiments with those from previously reported ECD experiments[32] is shown in Figure 8, in which differences between the *apparent* internal energy deposited by ECID and the average energy deposited by ECD as a function of the cluster ion size are compared.

For small clusters ($n \leq 21$), the apparent internal energy deposition in ECID is lower than the average energy deposited in ECD by up to 1.9 eV. The observed relative internal energy depositions are comparable for cluster sizes between $n = 21$ and $n = 25$, but higher internal energy deposition occurs for ECID at larger cluster sizes. This trend in relative energy deposition is opposite that expected from a kinetic shift effect and indicates that more internal energy is deposited for larger clusters in ECID. This effect is directly attributable to collisional energy transfer, which does not occur for ECD in which a free electron is captured.

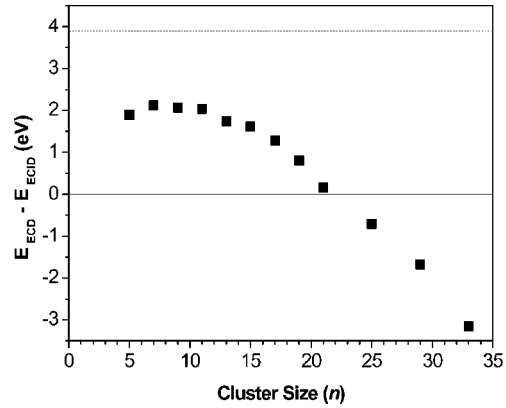

Figure 8. Energy difference, $E_{ECD} - E_{ECID}$, between the average numbers of water molecules lost from both pathways I and II combined in ECD[32] vs ECID of $Ca^{2+}(H_2O)_n$ with a Cs target using water binding energies calculated from a discrete implementation of the Thomson liquid drop model and quantum chemical values (see the text). The dashed line is the first ionization energy of cesium.

Effects of Ion Identity. To determine the effect of the metal ion identity upon energy transfer in ECID, analogous experiments were performed using hydrated divalent magnesium clusters for $n = 3-11$. For clusters in this size range, the maximum water loss, the minimum water loss, the average number of water molecules lost, and the branching ratio between the two pathways are essentially the same as those for Ca. ECD spectra for clusters containing either of these two alkaline-earth-metal dications are also very similar. These data suggest that an ion−electron pair is formed in the reduced clusters that do not lose a hydrogen atom.[32,47]

Conclusion

Ion nanocalorimetry is used to investigate the energy deposition that occurs in femtosecond collisions between charged nanodrops containing divalent Ca and Mg with either Cs or Ne atoms. Fragment ions formed by loss of water molecules from the doubly charged precursor as well as fragment ions formed by electron transfer from Cs are observed. The latter ECID process results in fragmentation from the reduced precursor by two competitive pathways corresponding to either exclusive loss of water molecules or loss of a H atom accompanied by water molecule loss. The internal energy deposition upon ECID is very broad and can be very high; ions with threshold formation energies above 16 eV are observed. Because of the significant kinetic shift for the larger clusters in these experiments, the actual energy deposition required to form these fragment ions on the microsecond time scale of these experiments can be substantially higher.

A sudden change in reactivity with cluster size occurs at $n \approx 20$, where the minimum number of water molecules lost by the hydrogen atom loss pathway jumps from zero for $n = 19$ to five for $n = 20$. Although the effects of formation of a third solvation shell may play a role in these results, a more thorough theoretical examination of the dynamics of the electron capture process for clusters in this size range may provide a better understanding of this phenomenon.

The differences between the ECID and ECD data for these nanodrops can be attributed to differences in energetics associated with capture of a free electron vs a bound electron from a neutral atom. The latter should result in less internal energy

deposition owing to the energy required to ionize the target gas, but this effect is counteracted by the additional energy that can be transferred in the collision event. Unlike ECD, the spread in internal energy deposition caused by the collision in the ECID process results in a very broad range of product ions that can have vastly different appearance energies. Finally, the time scales of the ECD and ECID experiments are significantly different, which results in a large kinetic shift for ECID unlike ECD experiments, which have time frames that are many orders of magnitude longer.

It is remarkable that, despite the significant differences between the internal energy deposited in ECID and ECD, spectra of small peptide ions obtained by these two methods are so similar.[15−18] From further comparisons of ECID and ECD spectra of different ion species, it may be possible to obtain information about the role of different electronic excited states in electron capture fragmentation pathways.

Acknowledgment. We acknowledge generous financial support from the European Project ITS-LEIF (Grant RII 3/02 6016), the Danish Natural Science Research Council (Grants 21-04-0514 and 272-06-0427), Carlsbergfonden (Grant 2006-01-0229), Lundbeckfonden, (A.I.S.H., P.H., M.K.L., and S.B.N.), the University of Aarhus, Denmark, for a Visiting Professor Fellowship (E.R.W.), and the National Institutes of Health (Grant ROI GM 064712; E.R.W. and W.A.D.).

References and Notes

(1) Zaia, J.; Biemann, K. *J. Am. Soc. Mass Spectrom.* **1994**, *5*, 649–654.
(2) Zhang, M. Y.; Wesdemiotis, C.; Marchetti, M.; Danis, P. O.; Ray, J. C.; Carpenter, B. K.; McLafferty, F. W. *J. Am. Chem. Soc.* **1989**, *111*, 8341–8346.
(3) McLafferty, F. W. *Science* **1990**, *247*, 925–929.
(4) Terlouw, J. K.; Kieskamp, W. M.; Holmes, J. L.; Mommers, A. A.; Burgers, P. C. *Int. J. Mass Spectrom. Ion Processes* **1985**, *64*, 245–250.
(5) Hudgins, D. M.; Raksit, A. B.; Porter, R. F. *Org. Mass Spectrom.* **1988**, *23*, 375–380.
(6) Wesdemiotis, C.; McLafferty, F. W. *Chem. Rev.* **1987**, *87*, 485–500.
(7) Hao, C.; Seymour, J. L.; Turecek, F. *J. Phys. Chem. A* **2007**, *111*, 8829–8843.
(8) Wesdemiotis, C.; Feng, R.; Williams, E. R.; McLafferty, F. W. *Org. Mass Spectrom.* **1986**, *21*, 689–695.
(9) Schalley, C. A.; Hornung, G.; Schroder, D.; Schwarz, H. *Int. J. Mass Spectrom.* **1998**, *173*, 181–208.
(10) Bowie, J. H. *Int. J. Mass Spectrom.* **2001**, *212*, 249–265.
(11) Turecek, F. *Mod. Mass Spectrom.* **2003**, *225*, 77–129.
(12) McAnoy, A. M.; Dua, S.; Schroder, D.; Bowie, J. H.; Schwarz, H. *J. Chem. Soc., Perkin Trans.* **2002**, *2*, 1647–1652.
(13) Zagorevskii, D. *Coord. Chem. Rev.* **2002**, *225*, 5–34.
(14) Fura, A.; Turecek, F.; McLafferty, F. W. *J. Am. Soc. Mass Spectrom.* **1991**, *2*, 492–496.
(15) Holm, A. I. S.; Hvelplund, P.; Kadhane, U.; Larsen, M. K.; Liu, B.; Nielsen, S. B.; Panja, S.; Pedersen, J. M.; Skrydstrup, T.; Støchkel, K.; Williams, E. R.; Worm, E. S. *J. Phys. Chem. A* **2007**, *111*, 9641–9643.
(16) Hvelplund, P.; Liu, B.; Nielsen, S. B.; Tomita, S.; Cederquist, H.; Jensen, J.; Schmidt, H. T.; Zettergren, H. *Eur. Phys. J. D* **2003**, *22*, 75–79.
(17) Hvelplund, P.; Liu, B.; Nielsen, S. B.; Tomita, S. *Int. J. Mass Spectrom.* **2003**, *225*, 83–87.
(18) Chakraborty, T.; Holm, A. I. S.; Hvelplund, P.; Nielsen, S. B.; Poully, J.-C.; Worm, E. S.; Williams, E. R. *J. Am. Soc. Mass Spectrom.* **2006**, *17*, 1675–1680.
(19) Hvelplund, P.; Liu, B.; Nielsen, S. B.; Panja, S.; Poully, J.-C.; Støchkel, K. *Int. J. Mass Spectrom.* **2007**, *263*, 66–70.
(20) Vekey, K.; Brenton, A. G.; Beynon, J. H. *Int. J. Mass Spectrom. Ion Processes* **1986**, *70*, 277–300.
(21) Breuker, K.; Oh, H. B.; Lin, C.; Carpenter, B. K.; McLafferty, F. W. *Proc. Nat. Acad. Sci. U.S.A.* **2004**, 101.
(22) Adams, C. M.; Kjeldsen, F.; Zubarev, R. A.; Budnik, B. A.; Haselmann, K. F. *J. Am. Soc. Mass Spectrom.* **2004**, *15*, 1087–1098.
(23) Garcia, B. A.; Siuti, N.; Thomas, C. E.; Mizzen, C. A.; Kelleher, N. L. *Int. J. Mass Spectrom.* **2007**, *259*, 184–196.
(24) Meng, F. Y.; Forbes, A. J.; Miller, L. M.; Kelleher, N. L. *Mass Spectrom. Rev.* **2005**, *24*, 126–134.
(25) Oh, H.; Breuker, K.; Sze, S. K.; Ge, Y.; Carpenter, B. K.; McLafferty, F. W. *Proc. Natl. Acad. Sci. U.S.A.* **2002**, *99*, 15863–15868.
(26) Zhang, X.; Guan, S. H.; Chalkley, R. J.; Recht, J.; Diaz, R. L.; Allis, C. D.; Marshall, A. G.; Burlingame, A. L. *FASEB J.* **2006**, *20*, A100.
(27) Iavarone, A. T.; Paech, K.; Williams, E. R. *Anal. Chem.* **2004**, *76*, 2231–2238.
(28) Cournoyer, J. J.; Lin, C.; Bowman, M. J.; O'Connor, P. B. *J. Am. Soc. Mass Spectrom.* **2007**, *18*, 48–56.
(29) Liu, H. C.; Häkansson, K. *J. Am. Soc. Mass Spectrom.* **2006**, *17*, 1731–1741.
(30) Turecek, F.; Syrstad, E. A. *J. Am. Chem. Soc.* **2003**, *125*, 3353–3369.
(31) Duncombe, B. J.; Duale, K.; Buchanan-Smith, A.; Stace, A. J. *J. Phys. Chem. A* **2007**, *111*, 5158–5165.
(32) Leib, R. D.; Donald, W. A.; Bush, M. F.; O'Brien, J. T.; Williams, E. R. *J. Am. Soc. Mass Spectrom.* **2007**, *18*, 1217–1231.
(33) Cooks, R. G.; Ast, T.; Kralj, B.; Kramer, V.; Žigon, D. *J. Am. Soc. Mass Spectrom.* **1990**, *1*, 16–27.
(34) Susič, R.; Lu, L.; Riederer, D. E., Jr.; Žigon, D.; Cooks, R. G.; Ast, T. *Org. Mass Spectrom.* **1992**, *27*, 769–776.
(35) Dejarme, L. E.; Cooks, R. G.; Ast, T. *Org. Mass Spectrom.* **1992**, *27*, 667–676.
(36) Kenttämaa, H. I.; Cooks, R. G. *Int. J. Mass Spectrom. Ion Processes* **1985**, *64*, 79–83.
(37) Hayakawa, S.; Kitaguchi, A.; Kameoka, S.; Toyoda, M.; Ichihara, T. *J. Chem. Phys.* **2006**, *124*, 24320.
(38) Hayakawa, S.; Minami, K.; Iwamoto, K.; Toyoda, M.; Ichihara, T.; Nagao, H. *Int. J. Mass Spectrom.* **2007**, *266*, 122–128.
(39) Dekrey, M. J.; Kenttämaa, H. I.; Wysocki, V. H.; Cooks, R. G. *Org. Mass Spectrom.* **1986**, *21*, 193–195.
(40) Griffiths, I. W.; Mukhtar, E. S.; March, R. M.; Harris, F. M.; Beynon, J. H. *Int. J. Mass Spectrom. Ion Processes* **1981**, *39*, 125–132.
(41) Baer, T.; Dutuit, O.; Mestdagh, H.; Rolando, C. *J. Phys. Chem. A* **1988**, *92*, 5674–5679.
(42) Chen, J. H.; Hays, J. D.; Dunbar, R. C. *J. Phys. Chem. A* **1984**, *88*, 4759–4764.
(43) Beranova, S.; Wesdemiotis, C. *J. Am. Soc. Mass Spectrom.* **1994**, *5*, 1093–1101.
(44) Donald, W. A.; Leib, R. D.; O'Brien, J. T.; Bush, M. F.; Williams, E. R. *J. Am. Chem. Soc.* **2008**, *130*, 3371–3381.
(45) Leib, R. D.; Donald, W. A.; Bush, M. F.; O'Brien, J. T.; Williams, E. R. *J. Am. Chem. Soc.* **2007**, *129*, 4894–4895.
(46) Leib, R. D.; Donald, W. A.; O'Brien, J. T.; Bush, M. F.; Williams, E. R. *J. Am. Chem. Soc.* **2007**, *129*, 7716–7717.
(47) Donald, W. A.; Leib, R. D.; O'Brien, J. T.; Holm, A. I. S.; Williams, E. R. *Proc. Nat. Acad. Sci. U.S.A.* [Online early access]. DOI: 10.1073/pnas.081549105.
(48) O'Brien, J. T.; Prell, J. S.; Holm, A. I. S.; Williams, E. R. *J. Am. Soc. Mass Spectrom.* **2008**, *19*, 772–779.
(49) Donald, W. A.; Williams, E. R. *J. Phys. Chem. A* **2008**, *112*, 3515–3522.
(50) Holland, P. M.; Castleman, A. W., Jr *J. Phys. Chem.* **1982**, *86*, 4181–4188.
(51) Boltalina, O. V.; Hvelplund, P.; Jørgensen, T. J. D.; Larsen, M. C.; Larsson, M. O.; Sharoitchenko, D. A. *Phys. Rev. A* **2000**, *62*, 023202.
(52) Larsson, M. O.; Hvelplund, P.; Larsen, M. C.; Shen, H.; Cederquist, H.; Schmidt, H. T. *Int. J. Mass Spectrom.* **1998**, *177*, 51–62.
(53) Stolterfoht, N. *Phys. Rep.* **1987**, *146*, 315–424.
(54) Blades, A. T.; Jayaweera, P.; Ikonomou, M. G.; Kebarle, P. J. *Chem. Phys.* **1990**, *92*, 5900–5906.
(55) Beyer, M. K. *Mass Spectrom.* **2007**, *26*, 517–541.
(56) Wong, R. L.; Williams, E. R. *J. Phys. Chem. A* **2003**, *107*, 10976–10983.
(57) McLafferty, F. W.; Wachs, T.; Lifshitz, C.; Innorta, G.; Irving, P. *J. Am. Chem. Soc.* **1970**, *92*, 6867–6880.
(58) Liu, B.; Haag, N. H.; Schmidt, H. T.; Cederquist, H.; Nielsen, S. B.; Zettergren, H.; Hvelplund, P.; Manil, B.; Huber, B. A. *J. Chem. Phys.* **2008**, *128*, 075102.

JP8019655